Renewable Energy 80 (2015) 664–673

Contents lists available at ScienceDirect

Renewable Energy

journal homepage: www.elsevier.com/locate/renene

On the design and tuning of linear model predictive control for wind turbines

Achin Jain [a, *], Georg Schildbach [b], Lorenzo Fagiano [c], Manfred Morari [d]

[a] Department of Mechanical and Process Engineering, ETH Zurich, Switzerland
[b] Model Predictive Control Laboratory, University of California Berkeley, USA
[c] ABB Switzerland Ltd., Corporate Research, Baden-Daettwil, Switzerland
[d] Automatic Control Laboratory, ETH Zurich, Switzerland

ARTICLE INFO

Article history:
Received 19 August 2014
Accepted 23 February 2015
Available online

Keywords:
Wind energy
Wind turbines
Model predictive control
Sensitivity analysis
Control system tuning

ABSTRACT

This paper presents a study on the design of linear model predictive control (MPC) for wind turbines, with a focus on the controller's tuning tradeoffs. A continuously linearized MPC approach is described and applied to control a 3-bladed, horizontal axis, variable speed wind turbine. The tuning involves a multiobjective cost function so that the performance can be optimized with respect to five defined measures: power variation, pitch usage, tower displacement, drivetrain twist and frequency of violating the nominal power limit. A tuning approach based on the computation of sensitivity tables is proposed and tested via numerical simulations using a nonlinear turbine model. The paper further compares the performance of the MPC controller with that of a conventional one.

1. Introduction

In the wake of increasing demands of wind energy, today the focus of research lies in maximizing the power output per unit investment. This would make wind energy more competitive with other sources of renewable energy. The production cost per unit of power decreases with an increase in size of the wind turbines, however the structure becomes more and more flexible. Thus, it is important to reduce the tower displacement and drivetrain twist in order to reduce the fatigue loads, hence eventually increasing the life span of the wind turbine. To achieve the best performance, the task of a controller becomes twofold: maximizing power output from the available wind and minimizing the fatigue of the turbine.

The classical method to control wind turbines makes use of several proportional-integral-derivative (PID) controllers. Some of them are effective in different regions of operation [1,2] and others are used for switching between these regions [3]. The gains of these controllers must be selected by considering aspects like power output, pitch actuation effort, tower fore-aft vibration and drivetrain twist. Another recent research focuses on individual pitch control (IPC) which uses different PID controllers for each blade. With the knowledge of local asymmetrical loading on turbines, it has been shown that the loads can be significantly reduced using IPC [4,5].

Controllers based on PID offer good performance but are not optimal. The current day research is focused more towards Gain Scheduled Linear Quadratic Regulator (LQR) [6,7], Feedback Linearization [8,9], H_2 & H_∞ Control [10–12], l_1 Control [13], Sliding Mode Control [14] and Model Predictive Control (MPC) [15–23], most of which are based on optimization principles. The fundamental advantage that optimization-based strategies offer is that the problem objective can be defined explicitly by putting weights on the relevant quantities we aim to limit, for instance: loads on tower, high speed shaft twist, power output from turbine etc.

In particular, MPC is a natural choice for a control algorithm for wind turbines because it is effective at handling multivariable systems with input and state constraints. Another potential advantage that MPC offers is its ability to predict behavior in future using a plant's model. Thus, it can use feedforward information to optimize the inputs while also considering the future states. If a prediction of the disturbances (wind) is also known through an estimation model [24], it further improves the controller's ability to reject these disturbances.

* Corresponding author.
E-mail addresses: ajain@student.ethz.ch (A. Jain), schildbach@berkeley.edu (G. Schildbach), lorenzo.fagiano@ch.abb.com (L. Fagiano), morari@control.ee.ethz.ch (M. Morari).

http://dx.doi.org/10.1016/j.renene.2015.02.057
0960-1481/

Several variants of MPC have been proposed for the problem of wind turbine control. In one of the earliest studies [16], linear MPC (LMPC) was successfully implemented on an onshore and an offshore wind turbine model. To account for the nonlinearities, which [16] did not, in Ref. [17] a scheduled MPC (SMPC) is designed, where the controller switches from one linear model to another depending on the operating point. Both SMPC and LMPC showed better speed control and load reduction in comparison to a baseline controller, at an expense of higher pitch usage. However, SMPC could perform better over LMPC only in speed control. In Ref. [18] it has been further illustrated that the performance of LMPC, continuously linearized MPC (CLMPC) and nonlinear MPC (NMPC) are comparable and not much better than a well-tuned PID controller. Thus, the linearized wind model very well captures the nonlinearities in the wind turbine. It is also seen that under perfect predictions of the wind speed, all the variants of MPC perform very well in load mitigation and speed control avoiding an increase of pitch activity when the turbine operates in the above rated region. The results for the perfect wind speed measurement are, however, not realistic. A more practical approach employs LIDAR to measure wind speed before the wind actually reaches the wind turbine [25]. In Ref. [19], Laks shows that even distorted measurements with LIDAR are better than having no preview at all. This result is also validated by Soltani [20] where mean wind speed estimated from LIDAR measurements is used as preview with LMPC. It exhibits load reduction and lower power fluctuation over a PID controller in extreme wind conditions. Koerber [21], Schlipf [22] and Spencer [23] have also shown that, in above rated conditions, MPC with knowledge of future wind condition helps to reduce loads significantly but the effect is most prominent when the wind is changing rapidly. While the literature discussed till this point deals with loads on the tower, [26] has demonstrated the use of MPC in reducing the blade fatigue loads.

From the above studies, it is evident that SMPC or CLMPC are sufficient to capture the nonlinear behavior of the wind turbine. The knowledge of future wind definitely gives MPC an edge over other control strategies, but the accuracy with which it can be measured and the cost surrounding measurement equipments remain issues that must still be resolved. On the other hand, while several publications indicated that MPC can be beneficial for wind turbine control, none of them discusses its tuning procedure. Indeed, tuning of MPC is a crucial part of the design and it might be a non-trivial task when multiple competing objectives are present, like in wind turbine control, such that a tradeoff between different performance measures has to be defined. To fill this gap in the literature, this paper discusses a tuning procedure for a continuously linearized model predictive controller by forming a meaningful objective function which explicitly accounts for 5 different performance indices. For the reasons discussed above, the paper primarily focuses on MPC without wind preview.

This paper is organized as follows. In section 2, a nonlinear model of the wind turbine is derived. In section 3, the simulation environment for MPC including the wind model, the performance indices and a baseline controller for comparison is described. In the following sections, the formulation of the model predictive controller is discussed together with a systematic approach to tune the control parameters. In section 6, qualitative and quantitative comparisons of MPC with a baseline controller are presented. Finally, the paper concludes with a discussion on the achieved results.

2. Model of the wind turbine

For the sake of this study, we consider a 3-blade horizontal axis pitch-regulated wind turbine. In particular, the parameters of the NREL 5 MW wind turbine [27], adapted from Ref. [16], are considered (see Appendix). The turbine model comprises the dynamics of 5 essential subsystems, as described in the following.

2.1. Aerodynamics

The momentum of the wind is transferred to the rotor by means of an aerodynamic torque, given by the relation

$$T_r = \frac{P_r}{\omega_r}, \tag{1}$$

where ω_r is the rotor speed and P_r is the equivalent power generated during the interaction of wind and turbine blades. P_r is a function of the wind speed v_w, blade radius R, air density ρ, and coefficient of performance C_p:

$$P_r = \frac{1}{2}\rho\pi R^2 v_w^3 C_p. \tag{2}$$

C_p is the ratio of power extracted by the wind turbine to power carried by the wind and is a function of blade pitch angle θ and tip speed ratio λ. The tip speed ratio is defined as

$$\lambda = \frac{v_w}{\omega_r R}. \tag{3}$$

The wind also exerts a thrust force F_t on the rotor and turbine which depends on the thrust coefficient C_t,

$$F_t = \frac{1}{2}\rho\pi R^2 v_w^2 C_t. \tag{4}$$

C_p and C_t are typically known from measurements. Their dependence on θ and λ is shown in Fig. 1 and Fig. 2.

2.2. Rotor mechanics

The transmission of power from rotor to generator is illustrated in Fig. 3. The wind produces an aerodynamic torque T_r on the rotor. The inertia of rotor and generator sides is represented by J_r and J_g, respectively. The low speed shaft is modeled as a flexible shaft with damping coefficient D_s and spring constant K_s. The shaft experiences twist δ due to varying torques on both ends. The gearbox couples the two rotating masses modeled as discs. $T_{d,r}$ and $T_{d,g}$ are the torques across the transmission whose gear ratio is indicated by N_g. The gearbox is assumed to have perfect mechanical efficiency. T_g is the resulting generator torque:

$$T_{d,g} = \frac{T_{d,r}}{N_g}. \tag{5}$$

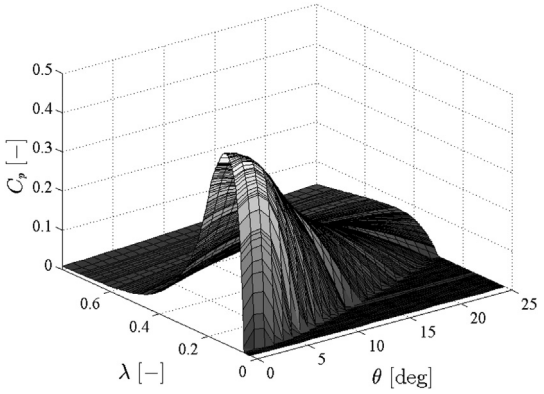

Fig. 1. Power coefficient, C_p.

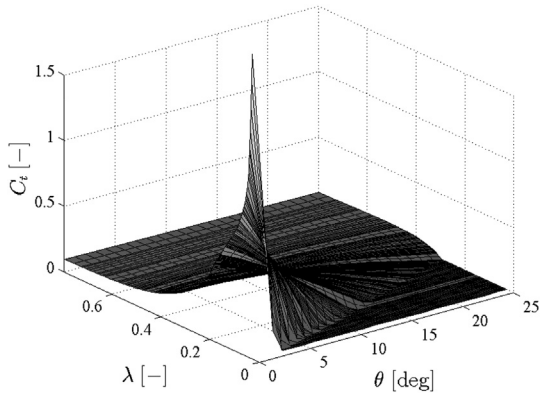

Fig. 2. Thrust coefficient, C_t.

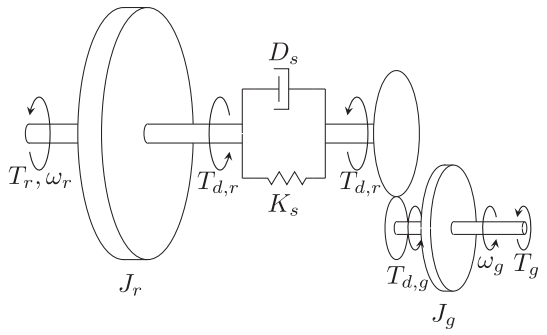

Fig. 3. Turbine mechanics [28].

Applying Newton laws of mechanics yields the following equations:

$$\dot{\omega} J_r = T_r - T_{d,r}, \tag{6}$$

$$\dot{\omega} J_g = T_{d,g} - T_g. \tag{7}$$

The governing equations for the drivetrain twist are:

$$T_{d,r} = D_s\dot{\delta} + K_s\delta, \tag{8}$$

$$\delta = \Omega_r - \frac{\Omega_g}{N}, \tag{9}$$

$$\dot{\delta} = \omega_r - \frac{\omega_g}{N}. \tag{10}$$

Ω_r and Ω_g represent angular position of the rotor and generator shaft, while ω_r and ω_g represent the corresponding angular velocities.

2.3. Tower dynamics

Due to the variability of the thrust force F_t, the tower exhibits fore and aft motion whose displacement ξ is modeled assuming a spring-mass-damper system:

$$M_t\ddot{\xi} + D_t\dot{\xi} + K_t\xi = F_t. \tag{11}$$

M_t, D_t and K_t are the mass, damping constant and spring constant of the tower, respectively. The motion of the tower changes the relative wind speed v_w^r at the rotor by the velocity of tower $\dot{\xi}$:

$$v_w^r = v_w - \dot{\xi}. \tag{12}$$

2.4. Generator dynamics

The generator is modeled as a first order system with time constant τ_T:

$$\dot{T}_g = -\frac{1}{\tau_T}T_g + \frac{1}{\tau_T}T_{g,\mathrm{ref}}. \tag{13}$$

Here, $T_{g,\mathrm{ref}}$ is the demanded torque and T_g is the output torque. The losses in transmission have been assumed to be zero. Therefore, the power output P_e is given by

$$P_e = T_g\omega_g. \tag{14}$$

2.5. Pitch actuation

The pitch is controlled collectively. The pitch actuator is assumed to follow second order dynamics:

$$\ddot{\theta} + 2\zeta\omega_n\dot{\theta} + \omega_n^2\theta = \omega_n^2\theta_{\mathrm{ref}}. \tag{15}$$

Here, θ_{ref} and θ are the demanded and actual pitch angles, respectively, ζ denotes the damping of pitch actuator and ω_n denotes the natural frequency of the actuator.

2.6. Steady state solution

Overall, the model has eight states $x := \left[\omega_r, \omega_g, \delta, \xi, \dot{\xi}, \theta, \dot{\theta}, T_g\right]^T$, two controllable inputs u: $= [\theta_{\mathrm{ref}}, T_{g,\mathrm{ref}}]^T$ and one uncontrollable input (disturbance), v_w. The state space representation of the nonlinear model is given by the following nonlinear ordinary differential equations:

$$\begin{aligned}
\dot{\omega}_r &= \frac{P_r(\omega_r, \theta, v_w^r)}{\omega_r J_r} - \frac{\omega_r D_s}{J_r} + \frac{\omega_g D_s}{J_r N_g} - \frac{\delta K_s}{J_r},\\
\dot{\omega}_g &= \frac{\omega_r D_s}{J_g N_g} - \frac{\omega_g D_s}{J_g N_g^2} + \frac{\delta K_s}{J_g N_g} - \frac{T_g}{J_g},\\
\dot{\delta} &= \omega_r - \frac{\omega_g}{N_g},\\
\ddot{\xi} &= -\frac{K_t}{M_t}\xi - \frac{D_t}{M_t}\dot{\xi} + \frac{1}{M_t}F_t(\omega_r, \theta, v_w^r),\\
\ddot{\theta} &= -\omega_n^2\theta - 2\zeta\omega_n\dot{\theta} + \omega_n^2\theta_{\mathrm{ref}},\\
\dot{T}_g &= -\frac{1}{\tau_T}T_g + \frac{1}{\tau_T}T_{g,\mathrm{ref}}.
\end{aligned} \tag{16}$$

The nonlinear model (16) can be written in a compact form as:

$$\dot{x} = f(x, u, v_w). \tag{17}$$

A steady state solution ($\dot{x} = 0$) for this model can be calculated as a function of wind speed v_w; such solutions will be used in section 4.1 to linearize the model. Fig. 4 shows the optimal trajectory (i.e. the one that maximizes the generated power) for power output, rotor speed, tower displacement and pitch angle under steady state conditions. Tower displacement velocity and pitch rate are zero under steady state operation.

As it is well-known [2], the turbine operating range is usually divided in two subregions, the so-called Region 2 and Region 3. Region 2 is characterized by low wind speeds and below rated operation (here, between cut-in speed of 3 m/s and about 11 m/s, see

Fig. 4). The objective in this region is to extract as much power as possible by selecting optimal C_p. It can be seen in Fig. 4 that for a constant tip speed, C_p is maximum for $\theta = 0$ deg. So, the optimal pitch angle $\theta = 0$ deg is selected throughout this region, and only torque control is required. For the sake of simplicity, we do not consider explicitly the so-called Region $2\frac{1}{2}$, which is defined in between the Regions 2 and 3, where the wind turbine achieves the rated speed but still the power output is lower than the rated value. However, since in Region $2\frac{1}{2}$ the control objective and the control input are the same as in Region 2, i.e. power maximization and torque, respectively, the same MPC tuning as in Region 2 can be used.

Region 3 is characterized by high wind speeds, in this case greater than 11 m/s. In these conditions the operation can no longer continue at constant pitch angle, since the mechanical power needs to be limited in order not to exceed the generator's rated power. Thus, as the wind speed increases, the pitch angle must be increased so that the angle of attack, and hence the lift on the blades, decreases. The aim in this region is thus power limitation.

3. Performance criteria and baseline controller

3.1. Wind model

Wind speed profiles were generated using a dynamic wind simulator, based on [15]. With a specified mean wind speed, wind direction, and turbulence level, the simulator provides a statistical wind model that closely approximates the wind profiles that a rotor would experience in reality.

We used the simulator to generate several cases with different mean wind speeds perpendicular to the face of rotor, both in Regions 2 and 3 for tuning our MPC control parameters. As regards the estimation of the effective rotor wind speed, required by the considered MPC strategy, a comprehensive review on this problem and on the related approaches that exploit available measurements can be found in Ref. [24].

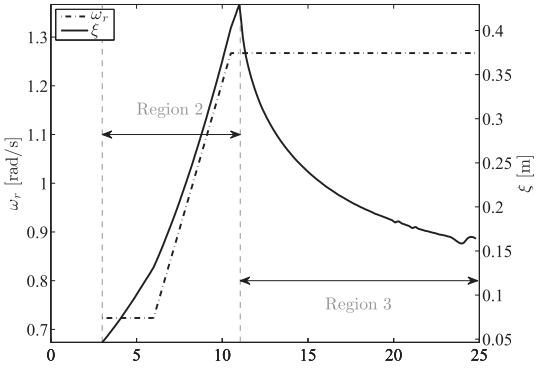

(a) Rotor Speed and Tower Displacement

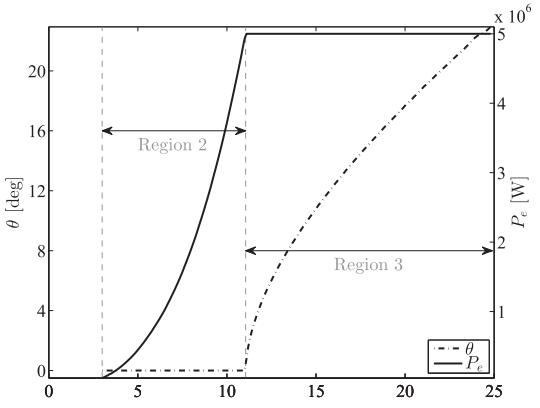

(b) Power Output and Pitch Angle

Fig. 4. Optimal trajectory under steady state conditions with v_w [m/s] on x-axis.

3.2. Performance criteria

We consider five indices to evaluate the performance of the controller:

3.2.1. Average power output/power variation (W)

For Region 2, an important performance criterion is the mean power output over a given time interval T,

$$AP = \sum_{t=1}^{T} \frac{P_e(t)}{T}. \tag{18}$$

The higher the value of AP, the better the controller's performance.

In Region 3, the performance criterion of interest is the root mean square value of the deviation of the generated power from the rated power output

$$PV = \left(\frac{\sum_{t=1}^{T} \left(P_e(t) - P_{e,\text{nom}}\right)^2}{T} \right)^{\frac{1}{2}}. \tag{19}$$

The lower the value of PV, the better the controller's performance.

3.2.2. Tower displacement (m)

It is desirable to minimize the displacements of the tower $\xi(t)$ from its steady state position $\tilde{\xi}(t)$ due to a changing wind speed. This quantity is taken as a measure of the tower fatigue caused by changing loads:

$$TD = \frac{\sum_{t=1}^{T} \left|\xi(t+1) - \tilde{\xi}(t)\right|}{T}. \tag{20}$$

3.2.3. Pitch usage (deg/s)

Rapid changes in pitch are undesirable, since they cause fatigue in the pitch actuator. Also, higher pitch activity can provoke vibrations in the structure if the resonance frequencies of the tower are excited [6]. Hence, the average pitch angle deviation during the considered time is computed:

$$PU = \frac{\sum_{t=1}^{T} \left|\theta_{\text{ref}}(t+1) - \theta_{\text{ref}}(t)\right|}{T}. \tag{21}$$

The lower PU, the better the controller's performance. This applies only to Region 3, since in Region 2 the pitch is always fixed.

3.2.4. Drivetrain twist rate (rad/s)

As another measure of loads, the following criterion is considered to account for the fatigue on the drivetrain shaft:

$$DT = \frac{\sum_{t=1}^{T} |\delta(t+1) - \delta(t)|}{T}. \tag{22}$$

This is also equivalent to considering the variability of the generator's torque, since the latter is closely related to drivetrain twist, see (8).

3.2.5. Frequency of power exceeding nominal

Only meaningful in Region 3, this criterion quantifies how many times the power exceeds the rated value:

$$PEN = \sum_{t=1}^{T} \chi(t), \tag{23}$$

$$\chi(t) = \begin{cases} 1, & \text{if } P_e(t) > P_{e,\text{nom}}, \\ 0, & \text{if } P_e(t) \le P_{e,\text{nom}}. \end{cases} \tag{24}$$

Clearly, it is not possible to obtain the best of every criterion, since for example a lower power variation usually implies a higher pitch usage. There is always a compromise which can be set by tuning the controller. The choice of the control approach influences what are the achievable tradeoffs (within the limits of what is physically possible) and how easy it is to tune the control law.

3.3. Baseline controller

To have a term of comparison for the MPC controller, a baseline controller is considered. The latter is a discrete-time controller with sampling time T_s, which is the same as that used by the MPC law. In particular, T_s is chosen such that the sampling frequency is greater than the frequency of the fastest pole of the linearized model (eigenvalue $\lambda_{\max}$ of A in (29)), in the considered case 14.15 rad/s. Thus, $T_s = 0.1\ s$ has been chosen here.

3.3.1. Region 2

The conventional controller used in Region 2 is torque-based control which tries to always operate the turbine at the most efficient power coefficient, C_p^*. λ^* is the corresponding tip speed ratio [2]:

$$T_{g,\text{ref}} = \frac{0.5\rho\pi R^5 \lambda^{*3} C_p^* \omega_r^2}{N_g}, \quad \theta_{\text{ref}} = 0. \tag{25}$$

3.3.2. Region 3

In Region 3, a PID controller is used. The pitch angle is controlled using proportional-integral-derivative action on error in rotor speed tracking:

$$\theta_{\text{ref}}(t) = K_p \omega_e(t) + K_i \int_0^t \omega_e(\tau)\mathrm{d}\tau + K_d \frac{\mathrm{d}\omega_e(t)}{\mathrm{d}t}, \tag{26}$$

$$\omega_e(t) = \omega_r(t) - \omega_{r,\text{nom}}. \tag{27}$$

The parameters K_p, K_i and K_d are designed using a similar methodology as in Ref. [29]. The generator torque is controlled by a feedback of the generator speed:

$$T_{g,\text{ref}}(t) = \frac{P_{e,\text{nom}}}{\omega_g(t)}. \tag{28}$$

The control signals of the PID controller are limited according to the input constraints that are present (discussed in section 4.3).

Equations (26–28) form the controller's structure. The values of K_p, K_i and K_d depend on the wind speed and can be designed by evaluating performance given by the five criteria introduced above, for a wide range of gains. For a particular wind scenario with mean wind speed of 15 m/s, Fig. 5 shows the dependence of performance on K_p and K_d. As a matter of fact, the integral gain does not have much influence on the performance, so that the value $K_i = 1$ was chosen such that the controller stabilizes the system for a wide range of K_p and K_d. The values for the latter have been selected (marked by * in Fig. 5) to achieve similarly good performance across all measures with slightly higher weight on power variation.

4. Design and tuning of linear model predictive control

The central idea behind using MPC [30] is to solve a finite time horizon optimal control problem in discrete time. The ability of MPC to handle actuator and state constraints, especially in MIMO systems, provides a potential advantage over traditional PID controllers. In this section, a linear MPC formulation for a wind turbine is derived, by defining the model, the cost function and the constraints. Once these ingredients have been set, the MPC law is implemented through a receding horizon strategy, where at the current time step only the first term of the solution sequence is applied to the plant, and at the next time step the whole optimal control problem is solved again, once the updated state variables have been measured.

4.1. Linearization

The turbine model (16) is continuously linearized at the current estimated wind speed $\tilde{v}_w$ to account for the nonlinear system behavior. The linearization makes LMPC computationally more tractable than NMPC. $\tilde{x}$ and $\tilde{u}$ represent corresponding steady state and steady input, respectively. Linearization of (17) can be expressed as

$$\dot{\hat{x}} = A(\tilde{v}_w)\hat{x} + B(\tilde{v}_w)\hat{u} + B_d(\tilde{v}_w)\hat{v}_w, \tag{29}$$

where

$$\hat{x} = x - \tilde{x}, \quad \hat{u} = u - \tilde{u}, \quad \hat{v}_w = v_w - \tilde{v}_w, \tag{30}$$

$$A(\tilde{v}_w) = \left.\frac{\partial f}{\partial x}\right|_{(\tilde{x},\tilde{u},\tilde{v}_w)}, \quad B(\tilde{v}_w) = \left.\frac{\partial f}{\partial u}\right|_{(\tilde{x},\tilde{u},\tilde{v}_w)}, \quad B_d(\tilde{v}_w) = \left.\frac{\partial f}{\partial v_w}\right|_{(\tilde{x},\tilde{u},\tilde{v}_w)}. \tag{31}$$

The linear model is then discretized with sampling time T_s by an explicit Euler method.

4.2. Cost function

The optimization is carried out with a quadratic cost function which is optimized at each time step:

$$J = \min_u \hat{x}_N P \hat{x}_N^T + \sum_{t=0}^{N-1} \hat{x}_t^T Q \hat{x}_t + \hat{u}_t^T R \hat{u}_t. \tag{32}$$

Q and R are diagonal, positive definite weight matrices that penalize the deviations from the steady state $\tilde{x}_t$ and steady input $\tilde{u}_t$, respectively, over a horizon length N which can be tuned for desired performance. For a finite horizon problem, a terminal cost $\hat{x}_N P \hat{x}_N^T$, $P > 0$ can be chosen such that feasibility is ensured at all times [30].

4.3. Constraints

The optimization is subject to constraints concerning both the states and the inputs. In particular, input constraints arise from actuator limitations: there is a limit on how much and how fast the blades can pitch. Similarly, the generator has a limitation on the maximum and minimum torque it can provide:

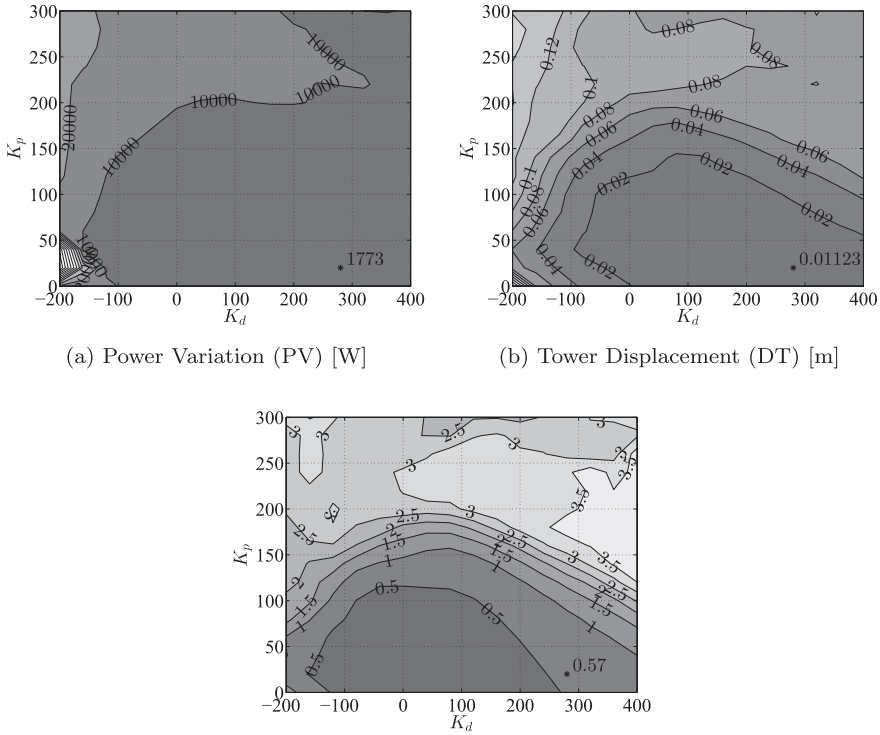

(a) Power Variation (PV) [W]

(b) Tower Displacement (DT) [m]

(c) Pitch Usage (PU)[deg/s]

(d) Drivetrain Twist Rate (DT) [rad/s]

(e) Power Exceeding Nominal Limit (PEN) [-]

Fig. 5. Performance of a conventional PID controller in Region 3 as a function of K_p and K_d for $K_i = 1$.

$$\theta_{\min} \leq \quad \theta \quad \leq \theta_{\max}, \tag{33}$$

$$\dot{\theta}_{\min} \leq \quad \dot{\theta} \quad \leq \dot{\theta}_{\max}, \tag{34}$$

$$T_{g,\min} \leq \quad T_g \quad \leq T_{g,\max}. \tag{35}$$

The strength of rotor assembly dictates the maximum rotational speed it can bear, and the minimum speed is dictated by the generator:

$$\omega_r \quad \leq \quad \omega_{r,\max}, \tag{36}$$

$$\omega_g \quad \geq \quad \omega_{g,\min}. \tag{37}$$

The input and state constraints mentioned above are hard constraints on the turbine operation. They must be followed strictly to avoid any damage to the wind turbine system. There are also soft constraints. For instance, when operating in Region 3, power should not vary much above the nominal power $P_{e,\text{nom}}$ because overcurrents/overvoltages can lead to thermal stresses [28]. So, imposing a power constraint is a reasonable approach to the problem:

$$\omega_g T_g \quad \leq \quad P_{e,\text{nom}}. \tag{38}$$

This constraint is a bilinear relation between two of the states which cannot be implemented as such in a linear optimization problem. So, the power constraint was linearized according to Fig. 6. This linearization is chosen such that it is tangent to the constant nominal power curve at nominal set point ($\omega_{g,\text{nom}}$,T_{nom}), which is a slightly conservative approximation. The area marked by dashed lines denotes the feasible region. The linear approximation (solid gray line in Fig. 6) is

$$\omega_{g,\text{nom}}^2 T_g + P_{e,\text{nom}} \omega_g \quad \leq \quad 2P_{e,\text{nom}} \omega_{g,\text{nom}}. \tag{39}$$

While in Region 3, (39) plays an important role; in Region 2 it always remains inactive.

5. Tuning procedure

The typical way to design the objective function is to look for the weights Q and R on states and inputs, respectively, that achieve a satisfactory performance, via a trial-and-error procedure. Such a procedure can be time-consuming and non-trivial, especially when many different aspects have to be balanced. We propose here a systematic approach to tune the MPC law, such that the procedure is easier and the interpretation of weights becomes more meaningful. This is done in two steps:

1) *Modifying the cost function to account explicitly for power maximization, and setting zero-terms in the weight matrix*

In Region 2, the aim is power maximization and in Region 3, power limitation. So, maximizing power in both regions superimposed with the power constraint (39) is an approach suitable for both regions. In the light of the above argument, the objective function can be augmented with a power maximization term, $x_t^T S x_t$ (compare equation (32)):

$$J = \min_u \hat{x}_N P \hat{x}_N^T + \sum_{t=0}^{N-1} \hat{x}_t^T Q \hat{x}_t + \hat{u}_t^T R \hat{u}_t - x_t^T S x_t, \tag{40}$$

where S is a positive semi-definite matrix, nonzero only for the terms corresponding to the product of ω_g and T_g in the state vector. This new term has a negative sign since the aim is to maximize power; moreover, since the generated power is a concave function of the state, the cost function J (40) is still convex. To this end, note that the new term accounts for the whole state x (and not only its deviation $\hat{x}$ from the linearization point $\tilde{x}$).

5.1. Region 3

Table 1 presents the sensitivity of the four performance measures for a wind profile in Region 3, if the objective function is based on (32). Unlike all the performance criteria listed in Table 1, the frequency of power exceeding the nominal value shows bidirectional behavior, in the sense that if it increases with increase in some weight, it might decrease when the same weight is further increased. So, it has been excluded in evaluating the sensitivity table. Nevertheless, this indicator provides useful insight while comparing PID with MPC. All the cost weights in (32) were initially set to $\frac{1}{\tilde{x}^2}$ or $\frac{1}{\tilde{u}^2}$ to normalize the contribution of each state and input to the cost function. This choice is referred to as "base weights" here. The weights were then increased (↑) or decreased (↓) by a factor α (10 in this case) one at a time, and Table 1 shows how much a performance measure changed when a specific weight was modified with respect to the base value. As a matter of fact, changing the weights on ω_r, ω_g, $\dot{x}_t$ and T_g did not change the performance significantly in any of the criteria. So, these terms are excluded from the cost function. The effect of input weights is not shown in the table for space limitations but the same behavior as the corresponding states has been observed. Excluding the redundant states from the cost function, (40) can be redefined with 4 states, 2 inputs and 1 power maximization term:

$$Q = \mathrm{diag}(0, 0, q_\delta, q_\xi, 0, q_\theta, q_{\dot{\theta}}, 0), \tag{41}$$

$$R = \mathrm{diag}\left(r_{\theta_{\mathrm{ref}}}, r_{T_{g,\mathrm{ref}}}\right). \tag{42}$$

The sensitivity analysis with this objective function is shown in Table 2. The weights which are the most favorable for performance are highlighted in **bold** and the most unfavorable in *italic*.

2) *Finding appropriate weights for non-zero terms in the cost function*

Once all the nonzero weight terms are identified, the next step is iterating between sensitivity tables defined at new set points, in order to find suitable values for such weights. For instance, Table 2 is calculated with respect to the base values. To reduce the pitch usage, the weight on $\dot{\theta}$ may be increased or θ may be decreased by a factor α. This forms a new base and a new sensitivity table can be calculated for it by again increasing and decreasing each weight by α. The local validity of the sensitivity table makes it necessary to recompute it again after a change has been made.

Table 2 also illustrates the trade-off between different performance measures. If the weight on the pitch rate is increased, pitch usage is reduced but power variation and tower displacement both increase. This effect can be explained by the fact that higher pitch rate weight restricts the actuator from quickly adjusting the pitch with the changing wind speed.

Table 2 has been calculated for mean wind speed of 15 m/s. Next, we analyze the correlation of this sensitivity table with another one calculated for different mean wind speed (18 m/s) in Table 3. A correlation matrix was calculated by dividing the corresponding sensitivity values from the two tables. The sensitivity values are very highly correlated for all the performance measures across all the weights. A negative correlation is observed only when the corresponding sensitivity values are very small, which is irrelevant anyways.

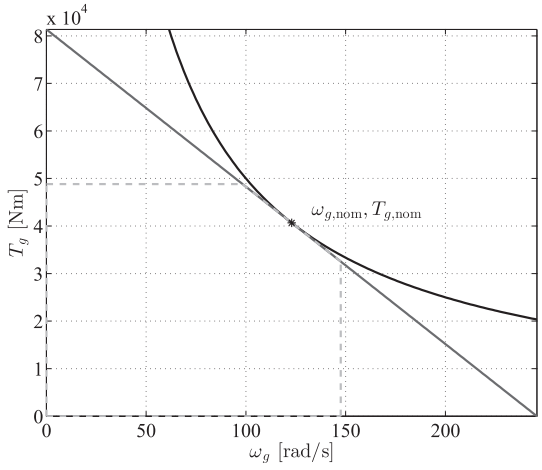

Fig. 6. Linearized power constraint with region of feasibility.

5.2. Region 2

In Region 2, only 3 performance measures are relevant: *PA*, *TD* and *DT*, because power output is always below nominal limit and the pitch is always fixed. A similar analysis (Table 4) in this region reveals that the sensitivity of these three measures on the weights is very low as compared to Region 3. Now, the contribution of tower displacement and tower velocity to performance becomes insignificant and therefore, ξ and $\dot{\xi}$ can be removed from the objective function. The weights on ω_r and ω_g have similar effects and can be assigned an equal weight. Again, after removing the redundant terms from the cost function, the Q and R matrices can be rewritten as:

Table 1
Sensitivity of performance measures on state weights with J(32) and base at steady state in Region 3.

Criteria	ω_r		ω_g		δ		ξ		$\dot{\xi}$		θ		$\dot{\theta}$		T_g	
	↑	↓	↑	↓	↑	↓	↑	↓	↑	↓	↑	↓	↑	↓	↑	↓
PV	5.26	0.00	5.05	0.00	1.06	0.25	22.22	0.00	1.95	−0.01	2.54	0.03	0.49	3.42	1.63	0.15
PU	0.05	0.00	0.05	0.00	0.05	0.00	22.38	−0.25	4.17	−0.04	13.82	−0.17	−0.98	3.20	0.05	0.00
TD	0.03	0.00	0.03	0.00	−0.07	0.00	−0.48	0.02	−0.03	0.00	−0.46	0.01	0.04	−0.41	0.03	0.00
DT	0.00	0.00	0.00	0.00	−0.04	0.01	2.24	0.00	0.07	0.00	0.03	0.00	0.00	−0.01	0.00	0.00

Table 2
Sensitivity of performance measures on state weights with J(40) and base at steady state in Region 3.

Criteria	P_e		δ		ξ		θ		$\dot{\theta}$	
	↑	↓	↑	↓	↑	↓	↑	↓	↑	↓
PV	−0.02	0.00	0.04	0.00	−0.25	0.04	**−0.42**	0.68	*0.82*	**−0.43**
PU	0.00	0.00	0.00	0.00	0.59	−0.06	0.26	−0.10	**−0.21**	*0.39*
TD	0.00	0.00	0.00	0.00	−0.07	0.01	**−0.09**	*0.09*	*0.11*	**−0.11**
DT	0.00	0.00	0.00	0.00	0.00	0.00	0.00	0.00	0.00	0.00

Table 3
Correlation of sensitivity between different wind scenarios, mean speed of 15 (m/s) and 18 (m/s).

Criteria	P_e		δ		ξ		θ		$\dot{\theta}$	
	↑	↓	↑	↓	↑	↓	↑	↓	↑	↓
PV	0.58	0.59	0.52	0.50	0.99	1.07	0.75	0.35	0.39	0.81
PU	1.42	1.41	24.33	14.58	1.86	1.88	0.77	0.71	1.16	1.31
TD	−2.52	−2.34	−3.12	−4.25	1.72	1.42	0.63	0.06	0.19	0.98
DT	0.20	−0.13	1.21	1.18	1.88	1.76	−0.36	−0.87	1.00	1.03

Table 4
Sensitivity of performance measures on state weights with J(32) and base at steady state in Region 2.

Criteria	ω_r		ω_g		δ		ξ		$\dot{\xi}$		T_g	
	↑	↓	↑	↓	↑	↓	↑	↓	↑	↓	↑	↓
AP	0.001	0.000	0.001	0.000	0.000	0.000	0.000	0.000	0.000	0.000	0.000	0.000
TD	−0.009	0.001	−0.009	0.001	−0.003	0.001	−0.001	0.000	0.000	0.000	0.004	−0.002
DT	−0.022	0.002	−0.022	0.002	0.074	−0.021	−0.003	0.000	0.002	0.000	0.042	−0.021

$$Q = \mathrm{diag}\left(q_\omega, q_\omega, q_\delta, 0, 0, 0, 0, q_{T_g}\right), \tag{43}$$

$$R = \mathrm{diag}\left(0, r_{T_{g,\mathrm{ref}}}\right). \tag{44}$$

As seen before, the inclusion of the generated power in the cost function helps to increase the power output. This is taken into account for further computations in section 6.

6. Results

In order to evaluate the performance of the MPC law tuned with the described approach, two simulation scenarios have been considered. The first one has mean wind speed of 8 m/s and turbulence of 7% which lies completely in Region 2 and the other one, lying in Region 3, has mean wind speed of 15 m/s and turbulence of 3%. The direction of the wind in both the scenarios is perpendicular to the surface of the rotor. Both the cases were simulated for 600 s with a time horizon of 2 s in MPC. As a matter of fact, the length of the prediction horizon has a small effect on the obtained performance when wind preview is not considered. Still, the use of MPC is advantageous due to the capability of handling constraints effectively and explicitly in the control design. The convex optimization problem was solved using Gurobi [31]. As shown by several contributions in the literature, the real-time implementation of the controller can be achieved reliably in practice, either by optimizing on-line [32,33] or by pre-computing off-line the corresponding explicit controller [34].

6.1. Region 2

The comparison of performance between MPC and that of the torque-based control in Table 5 shows that it is indeed difficult to outperform the latter, especially without preview. This result is also

Table 5
Performance comparison of MPC and PID in Region 2.

	AP [kW]	TD [m]	DT [rad/s]
Torque based	1763.8	0.0041	2.1e-5
MPC (Initial)	1719.8	0.0194	1.8e-4
MPC (Final)	1763.4	0.0040	1.7e-4

Table 6
Performance comparison of MPC and PID in Region 3.

	PV [W]	PU [deg/s]	TD [m]	DT [rad/s]	PEN [−]
PID	1407	0.53	0.0067	7.95e-5	2976
MPC (init.)	1863	1.07	0.0082	8.14e-5	958
MPC (final)	735	1.35	0.0066	8.14e-5	1936

Table 7
Sensitivity of performance measures on state weights with base at final tuning in Region 3.

Criteria	P_e		δ		ξ		θ		$\dot{\theta}$	
	↑	↓	↑	↓	↑	↓	↑	↓	↑	↓
PV	−0.01	0.00	0.01	0.00	−0.37	0.06	−0.61	0.68	*0.86*	**−0.63**
PU	0.00	0.00	0.00	0.00	*0.55*	−0.06	0.26	−0.11	**−0.22**	0.39
TD	0.00	0.00	−0.01	0.00	−0.13	0.02	−0.20	0.11	*0.15*	**−0.22**
DT	0.00	0.00	0.00	0.00	0.00	0.00	0.00	0.00	**0.00**	*0.00*

supported by Refs. [22,23]. This can be attributed to the fact that all the constraints in below rated conditions are inactive, and it is only in the presence of constraints that MPC is most effective. For MPC, the data in Tables 5 and 6 represent the absolute values of the performance indices calculated with base values and with tuned values for the cost weights, the latter obtained obtained after several iterations of the procedure described in section 5. With initial tuning, the baseline controller performs better in all the considered criteria. The final, tuned weights are such that a reasonable comparison can be made with the baseline controller, but there always exists a room for trade off between different performance measures.

The comparison was done for mean wind speed of 8 m/s. Quantitatively, both power output and tower displacement are more or less the same but the drivetrain twist rate is much larger with MPC (with tuned weights). Sensitivity on weights for the final tuning parameters can be used to further investigate the possibility of finding a different trade-off with MPC.

6.2. Region 3

Table 6 compares the performance of MPC against a PID controller which was tuned for a particular wind profile with mean wind speed of 15 m/s. With the base weight values, i.e. the initial tuning settings, MPC performed worse in 4 out of 5 criteria. Table 2 has then been used to tune MPC with the objective of reducing power variation. From the Table, one can see that the sensitivities of power variation with respect to increasing the weight on the pitch angle and decreasing the weight on the pitch rate are the most negative. Hence, we choose to increase the weight on the pitch angle. In subsequent steps, the weights on the power term and pitch angle were further increased to reach the final tuning where MPC performs better in 3 out of 5 criteria. In particular, the comparison shows that MPC performs much better in reducing the power variation and limiting the frequency of exceeding nominal power with final tuning. MPC can achieve almost half power variation while exceeding the nominal power only two-third times of PID (total simulation time steps are 600 s/T_s). Tower displacement in both the cases is very much comparable. The benefits with MPC come at an expense of higher pitch usage. Drivetrain displacement is very small in both cases but nonetheless, the PID controller performs slightly better in this criterion.

Table 7 shows the sensitivity of changing the weights for the final tuning. It suggests that a decrease in the pitch usage is possible by decreasing the weight on pitch angle or increasing the weight on pitch rate, but both of these would have an adverse effect on power variation as well as tower displacement. Also, Fig. 5-(a) suggests that the power variation that MPC is able to achieve seems unattainable with PID for any combination of gains. This shows the trade-off between different measures and it is an indication of the fact that MPC cannot outperform PID in all the measures simultaneously. However, the pitch usage with MPC is still much lower than the limits imposed by the pitch actuator.

7. Conclusions

The paper presented an approach for designing and tuning linear MPC for wind turbines. The performance of MPC can be very sensitive to cost weights which were selected by trading off five underlying criteria: Power Output/Power Variation, Tower Displacement, Pitch Usage, Drivetrain Twist Rate and Frequency of violating nominal power limit. These factors are very much related and there is always a compromise between them. It has been observed that even without preview, a well-tuned MPC, by means of multiobjective optimization, can outperform a conventional controller like PID in above rated conditions. However, in below rated conditions, MPC does not prove to be beneficial over the baseline torque-based control. Overall, the presented study indicates that a relatively systematic procedure can be set-up to properly tune the MPC controller, and that MPC can yield a higher flexibility than conventional controllers when the power output needs to be limited to a certain value. Considering the trend of modulating and controlling the power output of wind farms in order to meet grid stability requirements, this feature may prove to be crucially important in the next future.

Acknowledgment

The authors would like to thank Dr. Vedrana Spudić, Visiting Researcher at ETH Zurich, for providing us with wind simulator for generating effective wind speed.

Appendix. Model parameters

$$\rho = 1.225 \quad \left[\mathrm{kg}/\mathrm{m}^3\right]$$

$$P_{e,\mathrm{nom}} = 5e6 \quad [\mathrm{W}]$$

$$N_g = 97 \quad [-]$$

$$\omega_{r,\mathrm{nom}} = 1.26 \quad [\mathrm{rad/s}]$$

$$\omega_{g,\mathrm{nom}} = 122.91 \quad [\mathrm{rad/s}]$$

$$\omega_{g,\mathrm{min}} = 70.16 \quad [\mathrm{rad/s}]$$

$$J_r = 5.9154e7 \quad \left[\mathrm{kgm}^2\right]$$

$$J_g = 500 \quad \left[\mathrm{kgm}^2\right]$$

$$K_s = 8.7354e8 \quad [\mathrm{Nm/rad}]$$

$$D_s = 8.3478e7 \quad \left[\mathrm{kgm}^2/\mathrm{rad}/\mathrm{s}\right]$$

$$R = 63 \quad [\mathrm{m}]$$

$$H = 90 \quad [\mathrm{m}]$$

$$M_t = 4.2278e5 \quad [\mathrm{kg}]$$

$$K_t = 1.6547e6 \quad [\mathrm{Nm/rad}]$$

$$D_t = 2.0213e3 \quad \left[\mathrm{kgm}^2/\mathrm{rad}/\mathrm{s}\right]$$

$$\omega_n = 0.88 \quad [\mathrm{rad/s}]$$

$$\zeta = 0.9 \quad [-]$$

$$\tau_T = 0.1 \quad [\mathrm{s}]$$

$$\theta_{\min} = 0 \quad [\mathrm{deg}]$$

$$\theta_{\max} = 25 \quad [\mathrm{deg}]$$

$$\dot{\theta}_{\min} = -8 \quad [\mathrm{deg/s}]$$

$$\dot{\theta}_{\max} = 8 \quad [\mathrm{deg/s}]$$

References

[1] Bianchi FD, De Battista H, Mantz RJ. Wind turbine control systems: principles, modelling and gain scheduling design. Springer; 2006.
[2] Pao LY, Johnson KE. Control of wind turbines. Control Syst IEEE 2011;31(2):44–62.
[3] Fingersh LJ, Johnson KE. Baseline results and future plans for the NREL controls advanced research turbine. In: Proc. 23rd ASME wind energy symposium. Citeseer; 2004. p. 87–93.
[4] Bossanyi E. Further load reductions with individual pitch control. Wind Energy 2005;8(4):481–5.
[5] Bossanyi EA, Fleming PA, Wright AD. Validation of individual pitch control by field tests on two-and three-bladed wind turbines. Control Syst Technol IEEE Trans 2013;21(4):1067–78.
[6] Bossanyi E. Wind turbine control for load reduction. Wind Energy 2003;6(3):229–44.
[7] Boukhezzar B, Lupu L, Siguerdidjane H, Hand M. Multivariable control strategy for variable speed, variable pitch wind turbines. Renew Energy 2007;32(8):1273–87.
[8] Burkart R, Margellos K, Lygeros J. Nonlinear control of wind turbines: an approach based on switched linear systems and feedback linearization. In: Decision and control and European control conference (CDC-ECC), 2011 50th IEEE conference on. IEEE; 2011. p. 5485–90.
[9] Kumar A, Stol K. Simulating feedback linearization control of wind turbines using high-order models. Wind Energy 2010;13(5):419–32.
[10] Rocha R, Martins Filho L, Bortolus M. Optimal multivariable control for wind energy conversion system a comparison between h2 and h controllers. In: Proceedings of the 44th IEEE conference on decision and control, and the European control conference; 2005. p. 7906–11.
[11] Kristalny M, Madjidian D, Knudsen T. On using wind speed preview to reduce wind turbine tower oscillations. Control Syst Technol IEEE Trans 2013;21(4):1191–8.
[12] Ozdemir AA, Seiler P, Balas GJ. Design tradeoffs of wind turbine preview control. Control Syst Technol IEEE Trans 2013;21(4):1143–54.
[13] Schuler S, Schlipf D, Cheng PW, Allgower F. l_1-optimal control of large wind turbines. Control Syst Technol IEEE Trans 2013;21(4):1079–89.
[14] Corradini ML, Ippoliti G, Orlando G. Robust control of variable-speed wind turbines based on an aerodynamic torque observer. Control Syst Technol IEEE Trans 2013;21(4):1199–206.
[15] Sørensen P, Hansen AD, Rosas PAC. Wind models for simulation of power fluctuations from wind farms. J Wind Eng Ind Aerodyn 2002;90(12):1381–402.
[16] Henriksen LC. Model predictive control of a wind turbine [Ph.D. thesis]. Lyngby, Denmark: Technical University of Denmark, DTU, DK-2800 Kgs; 2007.
[17] Kumar A, Stol K. Scheduled model predictive control of a wind turbine. In: Proc. AIAA/ASME wind energy symp; 2009. pp. 2009–0481.
[18] Koerber A, King R. Nonlinear model predictive control for wind turbines. Proc EWEA.
[19] Laks J, Pao LY, Simley E, Wright A, Kelley N, Jonkman B. Model predictive control using preview measurements from lidar. In: Proc. 49th AIAA aerospace sciences meeting, Orlando, FL; 2011.
[20] Soltani M, Wisniewski R, Brath P, Boyd S. Load reduction of wind turbines using receding horizon control. In: Control applications (CCA), 2011 IEEE international conference on, IEEE; 2011. p. 852–7.
[21] Koerber A, King R. Combined feedback–feedforward control of wind turbines using state-constrained model predictive control. Control Syst Technol IEEE Trans 2013;21(4):1117–28.
[22] Schlipf D, Schlipf DJ, Kühn M. Nonlinear model predictive control of wind turbines using lidar. Wind Energy 2013;16(7):1107–29.
[23] Spencer MD, Stol KA, Unsworth CP, Cater JE, Norris SE. Model predictive control of a wind turbine using short-term wind field predictions. Wind Energy 2013;16(3):417–34.
[24] Soltani MN, Knudsen T, Svenstrup M, Wisniewski R, Brath P, Ortega R, et al. Estimation of rotor effective wind speed: a comparison. Control Syst Technol IEEE Trans 2013;21(4):1155–67.
[25] Wang N, Johnson KE, Wright AD. Comparison of strategies for enhancing energy capture and reducing loads using lidar and feedforward control. Control Syst Technol IEEE Trans 2013;21(4):1129–42.
[26] Castaignet D, Couchman I, Poulsen NK, Buhl T, Wedel-Heinen JJ. Frequency-weighted model predictive control of trailing edge flaps on a wind turbine blade. Control Syst Technol IEEE Trans 2013;21(4):1105–16.
[27] Jonkman JM, Butterfield S, Musial W, Scott G. Definition of a 5-MW reference wind turbine for offshore system development. Golden, CO: National Renewable Energy Laboratory; 2009.
[28] Burkart R. Nonlinear control of a wind turbine. Semester project, ETH Zürich.
[29] Hand MM, Balas MJ. Systematic controller design methodology for variable-speed wind turbines. Wind Eng Lond 2000;24(3):169–88.
[30] Mayne DQ, Rawlings JB, Rao CV, Scokaert PO. Constrained model predictive control: stability and optimality. Automatica 2000;36(6):789–814.
[31] Gurobi I. Optimization, Gurobi optimizer reference manual. 2014. http://www.gurobi.com.
[32] Wang Y, Boyd S. Fast model predictive control using online optimization. Control Syst Technol IEEE Trans 2010;18(2):267–78.
[33] Jerez J, Goulart P, Richter S, Constantinides G, Kerrigan E, Morari M. Embedded online optimization for model predictive control at megahertz rates. Autom Control, IEEE Trans 2014;59(12):3238–51.
[34] Alessio A, Bemporad A. A survey on explicit model predictive control. In: Nonlinear model predictive control. Springer; 2009. p. 345–69.